Forschungszentrum Karlsruhe
Technik und Umwelt

Wissenschaftliche Berichte
FZKA 5851

Neutrino Fluxes at KARMEN from Pion Decay in Flight

R. L. Burman
Institut für Kernpyhsik

November 1996

Forschungszentrum Karlsruhe
Technik und Umwelt
Wissenschaftliche Berichte
FZKA 5851

Neutrino Fluxes at KARMEN from Pion Decay in Flight

R. L. Burman[1,*]
Institut für Kernphysik

[1] *Permanent address: P-Division, Los Alamos National Laboratory, Los Alamos, New Mexico 87545, USA.*

Forschungszentrum Karlsruhe GmbH, Karlsruhe
1996

Forschungszentrum Karlsruhe GmbH
Postfach 3640, 76021 Karlsruhe

ISSN 0947-8620

Abstract

Calculations are presented for muon-neutrinos arising from charged pion decay in flight, and for possible (beyond-the-standard-model) neutrinos from pi-zero decay in flight. In-flight decays are calculated for both the ISIS spallation target and the μSR muon production target, with the neutrino fluxes evaluated at the center of the KARMEN detector. The calculated intensity of the (real) ν_μ-beam from π^+ decay is low, about 1.5 % of the decay-at-rest flux, so even though cross sections (e.g., neutral current excitation of ^{12}C) are larger due to higher neutrino energies, the additional rate represents an increase of only a few per cent. The calculated intensity and energy spectrum of ν's from π^0 decay will be needed for a search for the decay $\pi^0 \rightarrow \nu\ \nu$.

* *e-mail: burman@lampf.lanl.gov*

Neutrinoflüsse bei KARMEN aus Pionzerfällen im Fluge

Zusammenfassung

Berechnungen für ν_μ- Neutrinos, die sich aus Zerfällen im Fluge von geladenen Pionen ergeben, sowie mögliche (über das Standard Modell hinausgehende) Neutrinos aus dem π^0 - Zerfall im Fluge, werden dargestellt. Für das ISIS Spallationstarget und das μSR Myonen-Produktionstarget werden Zerfälle im Fluge mit ermittelten Neutrino-Flüssen im Zentrum des KARMEN Detektors berechnet. Die berechnete Intensität vom (realen) ν_μ - beam aus dem π^+ - Zerfall ist niedrig, etwa 1.5% des Flusses aus dem Zerfall in Ruhe, selbst wenn die Wirkungsquerschnitte (z.B. neutrale Stromanregung von ^{12}C) größer hinsichtlich höherer Neutrinoenergien sind, so zeigt die zusätzliche Rate einen Anstieg von nur wenigen Prozent. Das daraus bestimmte Intensitäts- und Energiespektrum von Neutrinos aus dem π^0 - Zerfall wird für die Suche nach dem Zerfall $\pi^0 \rightarrow \nu\ \nu$ benötigt.

1 Introduction

The KARMEN experiment has been designed around a neutrino source based upon π^+ and μ^+ decay-at-rest. These neutrinos are produced in the ISIS spallation target: the ν_μ from π^+ decay has an energy of 29.8 MeV, the ν_e and $\overline{\nu}_\mu$ from μ^+ decay have the 0-53 MeV Michel spectral shapes. In order to minimize neutron background, the KARMEN detector is sited at about 90^0 to the proton beam direction; the fast neutron flux from the spallation target is sharply peaked forward, while the neutrino flux from decay at rest is isotropic.

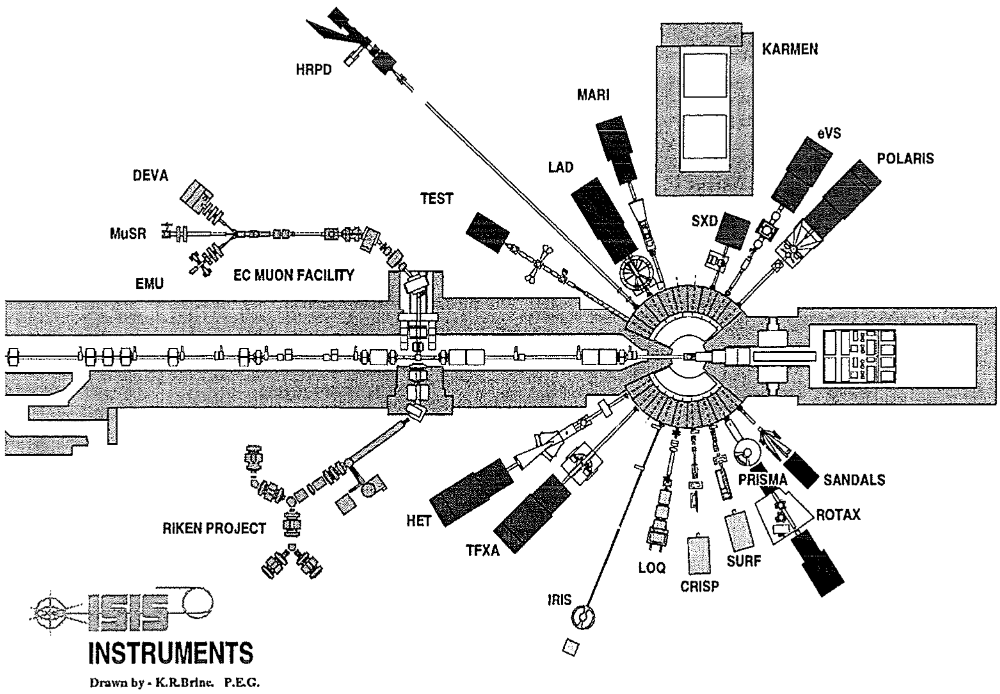

Figure 1: Floor layout of the ISIS neutron spallation facility. The 800 MeV proton beam enters from the left, intercepting first a μSR target and then the spallation target. The KARMEN blockhouse and detector are shown at $\approx 90^o$ to the proton beam and spallation target.

However, these are not the only neutrino sources. At the spallation target, about 2.5 π^+ mesons decay in flight for every 100 that decay at rest. The resulting ν_μ neutrinos from decay in flight have an energy spectrum extending to several hundred MeV, and are potentially (a) a background of μ^- from the reaction $^{12}C(\nu_\mu, \mu^-)X$, (b) a background source of neutral current excitation from the reaction $^{12}C(\nu_\mu, \nu_\mu{}')^{12}C^*$, and/or (c) a new neutrino beam.

An additional possiblity is that neutrinos have mass and can therefore exist with the "wrong" helicity: right-handed neutrinos or left-handed anti-neutrinos. This phenomenum could show up in the decay of the neutral pion to two neutrinos, $\pi^0 \rightarrow \nu\ \nu$. Here, one of the neutrinos would be right-handed, and KARMEN would detect the other (normal) neutrino or anti-neutrino. Another variant explanation would have the ν's being two separate species, e.g. $\nu_e\ \nu_\mu$, thereby violating lepton number conservation. The experimental signature in either case would be the production in the KARMEN detector of unexpected high-energy electrons or lower-energy muons. The experimental demonstration of such phenomena would, of course, be very exciting - the holy grail of physics beyond the standard model!

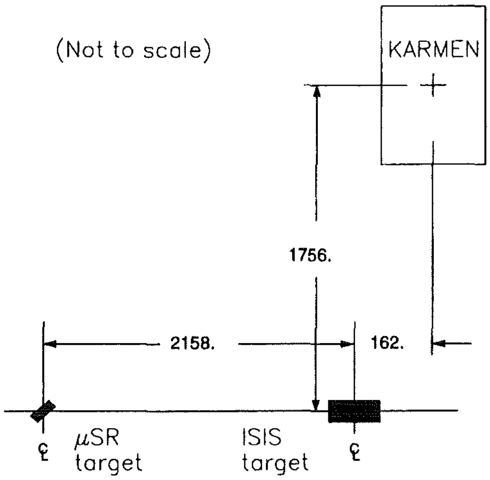

Figure 2: Schematic horizontal layout of the ISIS experimental area. The proton beam enters from the left, intercepting a μSR target and the spallation target. The relative positions of the two targets and the KARMEN detector are displayed. Dimensions are in cm.

In this report, absolute neutrino fluxes and spectral shapes are calculated for muon neutrinos from π^+ and π^- decay, and for neutrinos from π^0 decay. It is necessary to consider both the ISIS spallation target and the μSR target, since the latter, although thin, is at a more shallow angle to the detector. All neutrino fluxes are evaluated at the center of the KARMEN detector. It will be seen that the intensity of ν_μ's from π^+ decay in flight is low enough that this background rate is likely to be only a small correction to the prompt ν_μ-induced neutral current excitation of 12C.

Although the intensity of possible ν's from π^0 decay is not enough to establish new limits, it is enough to warrant a thorough analysis of the KARMEN data for this non-"standard model" decay.

2 Monte Carlo calculations

Neutrino fluxes for pion decay in flight were calculated with a Monte Carlo program[1, 2] that was designed for spallation targets or beam stop facilities at medium-energy proton accelerators. The program uses proton interaction cross sections, pion production and absorption cross sections, and particle transport to calculate neutrino fluxes.

Absolute normalization was provided by measurements[3] made on an instrumented mockup of a simplified beamstop; the event-by-event production of pions, followed by signals from pion and muon decay, was used to infer the rate of stopped π^+ production per incident proton. The code was then normalized, by 10% changes in the overall proton reaction and pion production cross sections, to give the measured stopped π^+ rate. This same code is used, in this report, to calculate for the KARMEN experiment the flux of ν_μ from π^+ decay-in-flight, and a flux of possible neutrinos from the decay $\pi^0 \to \nu\ \nu$.

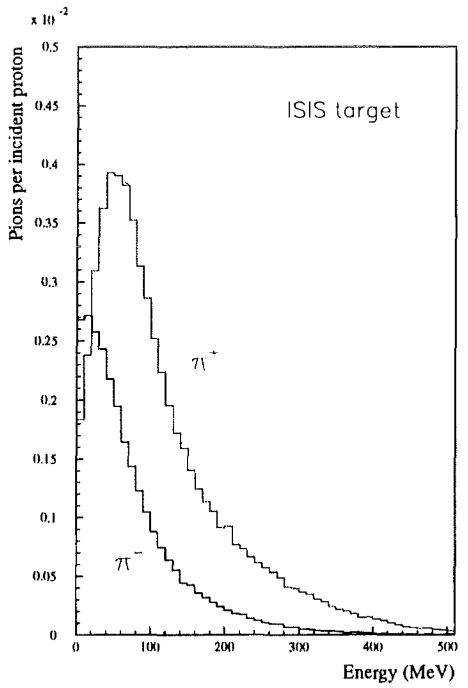

Figure 3: Energy spectra for π^+ and π^- produced in the ISIS tantalum spallation target. The spectrum for π^- is a much softer spectrum than that for π^+.

A layout view of the ISIS facility experimental area is displayed in Fig. 1. Beam lines for muon spin-resonance studies are shown exiting from the μSR target, and many neutron spectrometer facilities are shown radiating from the spallation target moderators. The 800 MeV proton beam, produced in a synchrotron, interacts first in a 5 mm carbon target (μSR target) and then in the massive tantalum target (ISIS spallation target). Neutrinos are produced in both targets, and can be detected via reactions on the carbon or hydrogen of the KARMEN liquid scintillation detector, which is sited in

Fig. 1 at right-angles to the spallation target. Relative positions of the KARMEN detector, the ISIS tantalum spallation target, and the μSR target are given quantitatively in the schematic layout in Fig. 2. It is seen that the KARMEN detector is at an angle of $\approx 85^o$ to the intersection of the proton beam and the ISIS target, and of $\approx 37^o$ to the intersection of the proton beam and the μSR target. The spatial dimensions of Fig. 2 serve to define the input geometry for the decay in flight part of the neutrino production code. The neutrino fluxes at the center of the detector are computed, as a weighted flux, for each step along the pion trajectory in order to improve the "statistical" accuracy of the Monte Carlo calculation.

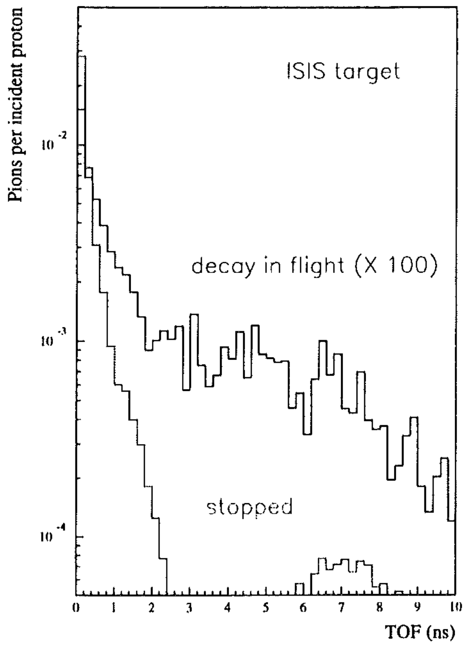

Figure 4: TOF spectra for π^+ produced in the ISIS tantalum spallation target. The lower histogram shows the TOF for charged pions that stop from ionization-loss mechanisms; the upper histogram shows the TOF for π^+ that decay in flight. The tails in both spectra for times greater than 2 ns are due to traversal of the less dense Be+water reflector.

A neutron spallation target facility consists of a spallation target assembly in close proximity to one or more neutron moderators, surrounded by a neutron reflector. The ISIS target facility has been modelled in some detail for neutrino production[2]. This model, as used for the present report, contains a target of tantalum plates separated by cooling water, surrounded by a Be+water reflector; inside the reflector, just above and below the tantalum target assembly, are four neutron moderators and neutron channels.

3 Neutrino Flux from π^+ Decay In Flight

Although the ISIS spallation target is (deliberately) designed to have as little empty space as possible, there are still pions that decay in flight before coming to rest. All π^0 that are produced, or that result from single charge exchange, will decay immediately ($\tau_o = 10^{-16}$ s) into two gamma rays or, possibly, two neutrinos. Charged pions are produced in the ISIS target with the energy spectra shown in Fig.3, where an integration over the angular distribution has been performed. The π^+ spectrum has a pronounced peak at about 50 MeV, with a long exponential tail extending to over 500 MeV; the π^- spectrum, as shown in Fig. 3, is much softer with the exponential fall-off starting at a low pion kinetic energy.

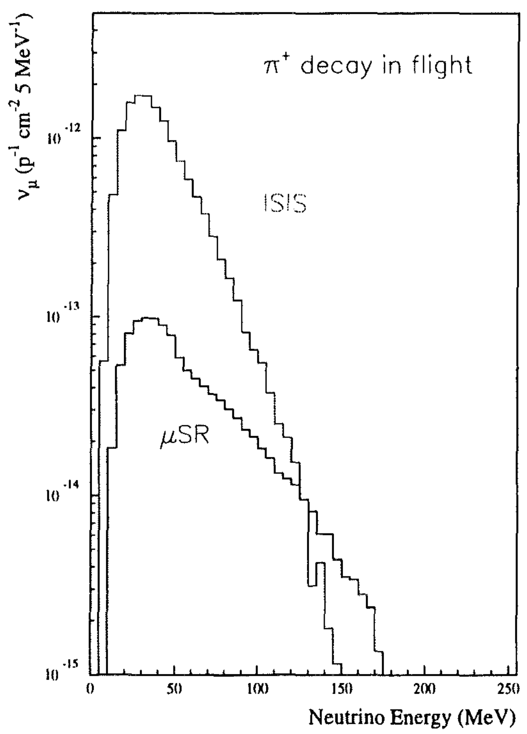

Figure 5: The energy spectra for the ν_μ fluxes for π^+ decay in flight. The neutrino flux from both the ISIS and μSR targets are displayed.

The typical time for these charged pions to stop is ≈ 2 ns; the actual time-of-flight (TOF) for π^+ in the ISIS tantalum target is shown in Fig.4. In the lower histogram the TOF for pions that stop is shown, where the small secondary peak at 7 ns is from pions stopping in the less dense Be+water reflector that surrounds the tantalum target. In the upper histogram is the TOF distribution for those π^+ that decay in flight. Again, the tail of decays at longer times comes from pions traversing the Be+water reflector.

Histograms of the calculated ν_μ fluxes from π^+ decay in flight are shown in Fig. 5. The ν_μ from the ISIS target are essentially below threshold for μ^- production, although

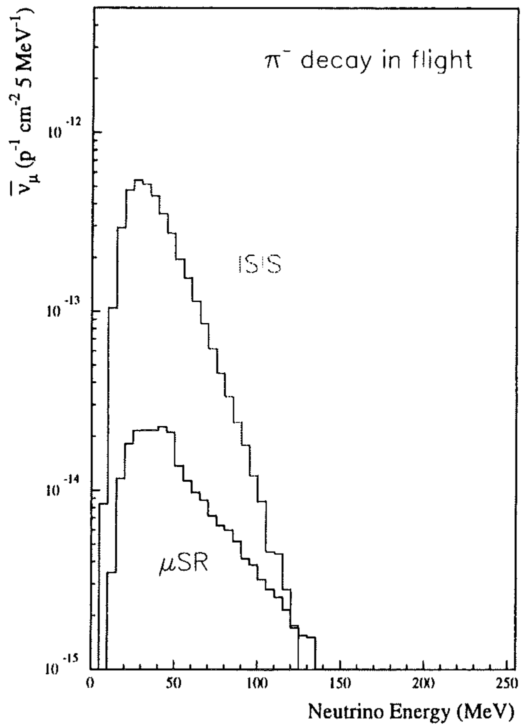

Figure 6: The energy spectra for the $\overline{\nu}_\mu$ fluxes for π^- decay in flight. The neutrino flux from both the ISIS and μSR targets are displayed.

still able to produce neutral current transitions. Both the intensity and the energy of the ν_μ are lowered significantly by the 90^0 position of the KARMEN detector relative to the proton beam. As shown in Fig. 5, the ν_μ flux from the μSR target, at a much shallower angle to the KARMEN detector, has a much harder spectrum; the intensity, however, is reduced by the small thickness of the carbon target. For the calculations in Fig. 5, the effective μSR target thickness was 7.07 mm of pyrolitic graphite (density 2.23 gm cm^3) corresponding to a 5 mm thick target at an angle of 45^0. These are the typical values for the μSR target; if other target thicknesses were used, the spectrum in Fig. 5 should be modified accordingly.

We can integrate the ν_μ flux from decay in flight (dif) to get the total flux at the center of the KARMEN detector,

$$\nu_\mu(dif) = 1.5 \times 10^{-11} \mathrm{p}^{-1} \mathrm{cm}^{-2}. \tag{1}$$

This can be compared to the flux from decay-at-rest neutrinos from the spallation target. The decay-at-rest intensity, for a tantalum target, is 0.045 ν p^{-1}. At the center of the KARMEN detector, 17.6 m from the ISIS source, the prompt decay-at-rest flux of ν_μ is $1.1 \times 10^{-9} \mathrm{p}^{-1} \mathrm{cm}^{-2}$. The ratio of the flux intensities is, therefore, about 1.5%. For decay-in-flight neutrinos of around 60 MeV the neutral current cross section is about twice the cross section for the Michel spectra decay-at-rest neutrino beam. However, the resultant event rate will still be less than 5% of the decay-at-rest beams.

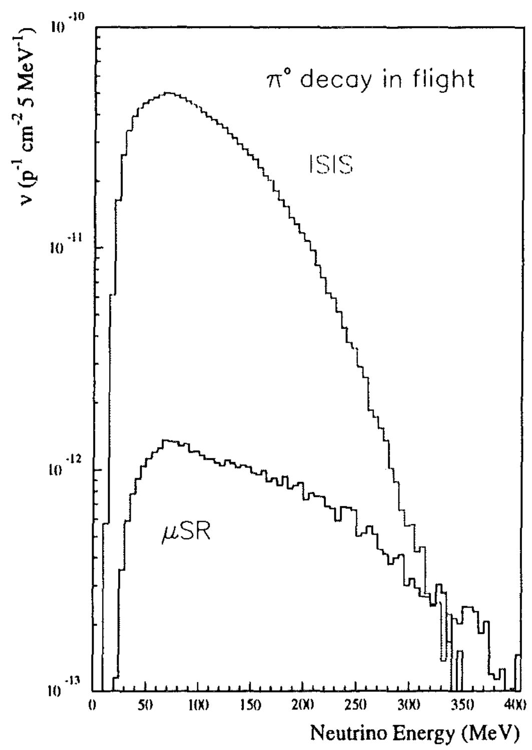

Figure 7: The energy spectra for the ν fluxes from the π^0 decay, $\pi^0 \to \nu\ \nu$, assuming that π^0 production has the same intensity and angular distribution as π^+ production. Spectra are shown for the ISIS and μSR targets separately.

In Fig. 6 we show the same neutrino energy spectra for the $\overline{\nu}_\mu$ from π^- decay in flight. The absolute intensity of the $\overline{\nu}_\mu$ flux is about 1/5 that of the ν_μ flux, and so will result in even fewer background events.

4 Neutrino Flux from $\pi^0 \to \nu\ \nu$ Decay

At a proton energy of 500-800 MeV, the production of pions is dominated by the 3/2-3/2 resonance in the pion-nucleon system. A comparison of statistical factors gives a much greater weight to π^+ and π^0 production than to π^- production; for a tantalum target, we would expect a ratio for π^+ /π^0 /π^- of 13.0/16.8/3.0 . A more realistic estimate can be made from a calculation of pion production at 800 MeV with the LAHET code system (see Ref. [4]), were we get an expected ratio of 13.0/9.0/3.1 .

For our calculation of π^0 production, we assume the same energy and angle distributions, and the same intensity, as for π^+; the intensity can be corrected by the last estimate given above. The Monte Carlo code proceeds by producing π^+ and then forcing them to decay immediately. In the pion center-of-mass, the full neutral pion mass is transmuted into two equal energy neutrinos. The code then uses the Lorentz boost, from the center-of-mass to the laboratory frame, to get the contribution to the neutrino

Table 1: Calculated neutrino fluxes for $\pi^0 \rightarrow \nu\ \nu$. The neutrino flux is computed at the center of the KARMEN detector, for π^0 production in the ISIS spallation target at $\approx 85^o$, and for π^0 production in the μSR target at $\approx 37^o$.

Threshold	Integral Flux	
	ISIS	μSR
(MeV)	(ν p^{-1} cm^{-2}	$\times\ 10^{-10}$)
0	12.80	.53
50	11.17	.50
60	10.25	.48
80	7.32	.40
100	6.41	.37
150	2.87	.26
200	.95	.17
250	.22	.10
300	.04	.05

intensity at the center of the KARMEN detector.

Neutrino fluxes from the hypothetical π^0 decay, $\pi^0 \rightarrow \nu\ \nu$, are shown in Fig. 7. The flux from the ISIS target shows a broad peak at around 70 MeV, and extends to above 300 MeV. The flux from the μSR target is considerably harder, but due to the thinner target (7.07 mm carbon, as projected perpendicularly to the proton beam) has a much lower intensity. Values of the integrated neutrino flux for π^0 decay in the two targets, as a function of the neutrino energy threshold, are listed in Table 1.

The sensitivity of the KARMEN experiment to $\pi^0 \rightarrow \nu\ \nu$, for the case where the neutrinos are ν_e, can be estimated by multiplying the neutrino spectrum in Fig. 7 by the cross section for the reaction $^{12}C(\nu_e, e^-)X$. A quick look suggests that the KARMEN experiment is close to the limits, from analyses of K-decay experiments[5] at the Brookhaven National Laboratory, that are listed in the Particle Data Group tables.

5 Flux Uncertainty

Estimates of the neutrino flux uncertainties for these caculations can be based upon the error analysis for the decay-at-rest fluxes as given in ref[1]. There, as discussed above, the absolute normalization of the code was provided by the E866 simplified beamstop experiment[3]. Because the code was normalized by the E866 data, there is no contribution to the uncertainty in the decay-at-rest flux from the measured pion production absolute normalization. The relative pion production cross section errors are folded into systematic effects in the E866 analysis. Error estimates from ref[2] for the present KARMEN experiment are given in Table 2.

Table 2: Estimated errors in the calculated neutrino fluxes from π^+ decay-at-rest and π^+ decay-in-flight.

Source of uncertainty	Decay-at-rest (%)	Decay-in-flight (%)
Fit of E866 data	2.4	-
Cross section error	-	9.5
Systematic effects in E866	5.9	5.0
ISIS simulation	2.0	5.0
Proton beam energy	0.3	0.3
Protons on target	2.0	2.0
Distance to detector	0.5	0.5
Quadrature sum	7.1	12.1

However, for the decay-in-flight neutrino fluxes presented in this report, there is no absolute normalization. As listed in Table 2, the main difference between the decay-in-flight and decay-at-rest uncertainties are in the absolute normalizations of the measured pion production cross sections. A normalization uncertainty for decay-in-flight is composed of both a 9.5% contribution from the absolute normalization errors quoted in the pion production experiments, and a 5.0% contribution from the E866 experiment. This latter number comes from the part of the "systematic effects in E866" entry in Table 2 that represents a change in the code normalization, but that does not involve the pion production cross section errors.

In addition, a larger number (5.0%) is used for the decay-in-flight flux simulation error. The number of pions that can decay in flight are quite sensitive to the modelling of low-density spaces in the spallation target assembly. The elements of the target in-line with the proton beam are quite well defined, but the moderator and shielding surrounding the target are not so well described. Therefore, computer runs were made with movements of various of the moderator and shielding components. Typically, for a movement of 2.5 cm, the decay-in-flight flux changed up to 8%. A reasonable estimate of the "likely" flux uncertainty from the open space uncertainty is 4.5%; this, folded with the 2.0% uncertainty from component simulation, results in the 5% entry under "ISIS simulation" in Table 2.

6 Summary

Calculations of the decay-in-flight neutrino fluxes for the KARMEN experiment have been presented. Neutrino fluxes were computed for pion production at both the ISIS and the μSR targets, and evaluated at the center of the KARMEN detector. The ν_μ and

$\overline{\nu}_\mu$ fluxes, from charged pion decay, were given in graphical form. The ν fluxes that might be present from a non-standard-model π^0 decay, $\pi^0 \to \nu\ \nu$, were given in both graphical and tabular form.

7 Acknowledgements

We gratefully acknowledge financial support from the Forschungszentrum Karlsruhe (Germany). We also thank A. Benen and J. Rapp for useful discussions about the results of these calculations.

References

[1] R.L. Burman, M.E. Potter and E.S. Smith, Nucl. Instr. and Methods **A291** (1990) 621.

[2] R.L. Burman, A.C. Dodd and P. Plischke, Nucl. Instr. and Meth. in Phys. Res. A 368 (1996) 416.

[3] R.C. Allen, *et al.*, Nucl. Instr. and Methods **A284** (1989) 347.

[4] R.L. Burman and P. Plischke, Forschungszentrum Karlsruhe report, FZKA 5834 (1996).

[5] M.S. Atiya, *et al.*, Phys. Rev. Letters **66** (1991) 2189; Cyrus M. Hoffman, Phys. Lett. **B 208** (1988) 149.